LETTERS
https://doi.org/10.1038/s41566-021-00823-w

nature photonics

OPEN

Coexistence of dynamical delocalization and spectral localization through stochastic dissipation

Sebastian Weidemann[1,4], Mark Kremer[1,4], Stefano Longhi[2,3] and Alexander Szameit[1]✉

Anderson's groundbreaking discovery that the presence of stochastic imperfections in a crystal may result in a sudden breakdown of conductivity[1] revolutionized our understanding of disordered media. After stimulating decades of studies[2], Anderson localization has found applications in various areas of physics[3–12]. A fundamental assumption in Anderson's treatment is that no energy is exchanged with the environment. Recently, a number of studies shed new light on disordered media with dissipation[14–22]. In particular it has been predicted that random fluctuations solely in the dissipation, introduced by the underlying potential, could exponentially localize all eigenstates (spectral localization)[14], similar to the original case without dissipation that Anderson considered. We show in theory and experiment that uncorrelated disordered dissipation can simultaneously cause spectral localization and wave spreading (dynamical delocalization). This discovery implies the breakdown of the commonly known correspondence between spectral and dynamical localization known from the Hermitian Anderson model with uncorrelated disorder.

In the famous Drude model[23], electronic conductivity relies on the idea that moving electrons, understood as particles, are decelerated by random collisions with the positive ions of the crystalline lattice, resulting in a diffusive motion. The discovery of quantum mechanics showed that electrons exhibit wave characteristics[24]. Consequently, Anderson included wave interference in the treatment of electron dynamics and discovered an unexpected metal–insulator transition, that is, lattice disorder can induce a sudden halt in the spatial spreading of the electron wavefunction[1] (Fig. 1). Being general in its setting, Anderson's model also applies for systems beyond electrons in solids[25,26], such as electromagnetic waves[5,6], matter waves[27,28] and sound waves[29]. Both Drude's and Anderson's theories naturally assume conservation of energy and particle number within the system. However, most systems are dissipative and exchange energy or particles with their environment. A celebrated example of the interplay of disorder and an external energy exchange is Mott's $T^{-1/4}$ law for the conductivity of amorphous semiconductors at low temperatures[13]. Despite the presence of disorder, a phonon-assisted hopping between the localized electron states facilitates a spatial spreading of the electron wavefunction.

Recently, several studies provided new insight on this topic by proposing and theoretically analysing novel dissipative (that is non-Hermitian) settings of disordered systems[15–22,30]. These works suggest that the presence of dissipation in disordered systems leads to novel phenomena such as the tuneable localization of states[17] or the appearance of so called 'Anderson attractors'[31]. Broader attention was also paid to disorder in (open) finite-sized systems or systems with bulk absorption[21,32–34], where (for example) the presence of dissipation impairs the weak localization. Another example is the emergence of necklace states in such frameworks, which leads to anomalous transmission through delocalized states with relatively short lifetimes[19,35,36].

Whereas most of the previous works studied the influence of dissipation as an additional effect within an already disordered system, the wave dynamics in systems where the dissipation is not a mere addition but the source of disorder itself remain little discussed. Conversely, the presence of dissipation with a certain degree of randomness should be relevant for a multitude of real systems. Mathematically, the case of disordered (that is stochastic) dissipation can be described by random changes in the imaginary part of the potential and such a setting can represent a stochastic energy or particle exchange of the system with the environment. This setting also constitutes the direct non-Hermitian analogue[14] of the Hermitian Anderson model, as the randomness is transferred from the real part of the potential to its imaginary part. In the context of this work, we therefore dub this model the non-Hermitian Anderson model. Even though the mechanism of localization is qualitatively distinct and does not rely on the interference of multiple scattering paths[14], numerical results showed that disorder solely in the imaginary part of a potential can also lead to exponential localization of all eigenstates[14,20]. In a Hermitian system, under weak conditions[37] that are always satisfied for uncorrelated disorder[38], the pure point spectrum with exponential localization of all eigenstates (dubbed spectral localization) necessarily prevents wave spreading in the lattice; that is, spectral localization implies dynamical localization[38]. Only for certain correlated disorder, such as in the random dimer model[39], is wave spreading still possible in the presence of spectral localization[37]. Conversely, dynamical localization implies spectral localization independently of disorder correlations, as a consequence of the Ruelle–Amrein–Georgescu–Enss (RAGE) theorem. In open systems, where the dynamics is described by an effective non-Hermitian Hamiltonian or a master equation in Lindblad form, the complex nature of eigenvalues of the Hamiltonian or Lindbladian operators could break the correspondence between spectral and dynamical localization even for uncorrelated disorder, such that the physics of wave dynamics in a system with stochastic dissipation remains an exciting, yet largely open, question.

[1]Institute for Physics, University of Rostock, Rostock, Germany. [2]Dipartimento di Fisica, Politecnico di Milano, Milan, Italy. [3]IFISC (UIB-CSIC), Instituto de Fisica Interdisciplinar y Sistemas Complejos, Palma, Spain. [4]These authors contributed equally: Sebastian Weidemann, Mark Kremer. ✉e-mail: alexander.szameit@uni-rostock.de

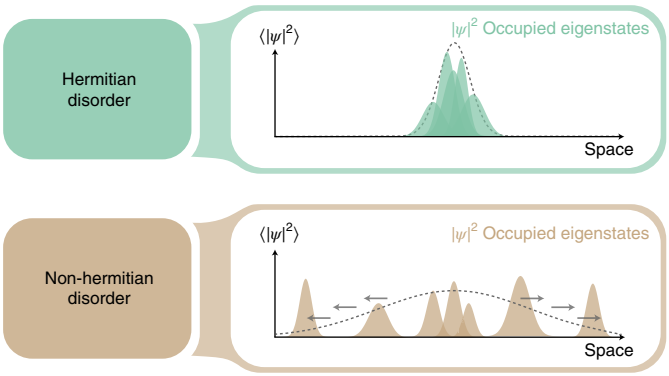

Fig. 1 | Localization and wave spreading in disordered lattices. Consider an initially localized single-particle wavefunction in an infinitely extended lattice with uncorrelated disorder. Top: in a Hermitian system, disorder can lead to Anderson localization, which is characterized by localized eigenstates and the average distribution $\langle|\psi|^2\rangle$ of the wavefunction remains localized around the initial position. Because only eigenstates close to the initial position are considerably populated, spatial spreading is suppressed. Bottom: in a system with random dissipation, that is, non-Hermitian disorder, the eigenstates can also become localized, yet dominantly occupied eigenstates can be found arbitrarily far away from the initial position. Hence $\langle|\psi|^2\rangle$ temporally broadens (dynamical delocalization), which is in strong contrast to the Hermitian case. The dashed lines schematically show the envelope of the wave packet, while grey arrows indicate the flow of excitation.

In this work, we show that the mere presence of uncorrelated static dissipation that is randomly distributed in a one-dimensional (1D) space leads to exponential localization of all eigenstates, but does not necessarily prevent wave spreading; that is, we show the breakdown of the correspondence between spectral and dynamical localization in the non-Hermitian Anderson model. This highly non-trivial result is deeply rooted in the stochastic distribution of the lifetimes of localized states in such a way that the localized eigenstate with the longest lifetime can be found statistically anywhere in the system. By using numerous different disorder realizations, we can extract and quantify not only the exponential localization, but also the spatial spreading. It is important to note that the non-Hermitian Anderson model fundamentally differs from Mott's considerations[13]: the exchange of energy or particles with the environment is included in our non-Hermitian Hamiltonian and the stochastic dissipation causes not only the spatial spreading, but simultaneously evokes spectral localization. Moreover, against all intuition, in the non-Hermitian Anderson model disorder in the real part of the potential is not required, as opposed to the Hermitian case. We formulate a theoretical model that can describe the observed dynamical delocalization by dynamic population changes of eigenstates that can be spatially separated by distances far beyond the localization length (Fig. 1). For strong disorder, our model also quantitatively captures the amount of spatial spreading. We experimentally verify our predictions in an optical system with controllable dissipation consisting of coupled optical fibre loops, where the light propagation corresponds to the time evolution of a single-particle wavefunction within a double-discrete 1 + 1D mesh lattice.

We start by developing an analytic model for the wave dynamics in a system with stochastic dissipation. Our approach considers a general, time-independent 1D lattice with ψ_n as the field amplitude at lattice site n. Anderson considered real lattice site potentials—that is, the Hermitian case—and found that for a random potential all eigenstates can become exponentially localized and, consequently, spatial spreading is prevented. In contrast, we consider complex potentials and the imaginary part of the potential randomly changes in space. This corresponds to the presence of dissipation that is randomly distributed on the lattice sites. The real part of the potential does not have to be disordered. To derive the wave dynamics, we also assume that all eigenstates are exponentially localized. While this assumption has been numerically predicted[14], we experimentally confirm the exponential localization in this work. To theoretically buttress this conjecture, we also analytically derive the spectral localization from the stochastic dissipation for a special case of the Hatano–Nelson model[15] (Supplementary Section 6).

When leaving the realm of Hermitian systems, the question of how the wave spreading may be defined arises, as the total probability is not a conserved quantity anymore. For instance, disentangling energy transport from energy exchange is a general problem of open systems. In all following considerations, we are therefore taking the position of an observer who has no a priori knowledge about the initial intensity or losses within the system. Hence, we follow the procedure of single-photon experiments in the field of non-Hermitian physics[40–42], where non-detection events (for example, the loss of photons due to dissipation) are not part of the statistics. Mathematically, this corresponds to a normalization of the total probability at each observation time.

In this approach, it is crucial to evaluate the relative population of eigenstates during the temporal evolution. Here, the stark contrast with the Hermitian case emerges, as the non-Hermitian character of the lattice causes the population of the eigenstates to change during evolution, even for an infinitely extended lattice. Consequently, the mere fact that all eigenstates are localized does not necessarily hinder spatial spreading. We show this by considering the eigenvalue spectrum. After exciting the lattice with a single-site excitation, the population of the states is determined by weight factors that are governed by the overlap between the initial single-site excitation and the exponentially localized eigenstates. Hence, a weight factor is proportional to $\exp(-d/l_c)$, where d is the distance between the excited site and the centre of the state, and l_c the localization length of the exponentially localized state (Fig. 2a). Moreover, due to the random character of the lattice, the weight factor of each eigenstate j experiences a phase oscillation of the form $\exp(-i\mathrm{Re}(\lambda_j)t)$, where λ_j is the eigenvalue of the corresponding state at time t. As all eigenvalues of the eigenstates possess different imaginary parts, the weight factor of each state is also modified by a term $\exp(\mathrm{Im}(\lambda_j)t)$, such that its population, relative to other eigenstate, changes over time. Let us assume that at time $t=0$ primarily the eigenstate with eigenvalue $\lambda_0 \in \mathbb{C}$ is excited, whereas the weight factor of another state, with eigenvalue λ_d and localization centre at position d, is smaller by the factor $\exp(-d/l_c)$. Since the imaginary part can be associated with the decay rate of the eigenstate, one can conclude that if $\mathrm{Im}(\lambda_d) > \mathrm{Im}(\lambda_0)$, then the state with eigenvalue λ_d, corresponding to a lower decay rate, will become dominant at a time t_{change}, which is given by

$$\exp(-d/l_c)\exp((\mathrm{Im}(\lambda_d) - \mathrm{Im}(\lambda_0))t_{\mathrm{change}}) \approx 1. \quad (1)$$

At this point, for $t > t_{\mathrm{change}}$, the weight factor of the eigenstate with eigenvalue λ_d exceeds that of the initially excited eigenstate with eigenvalue λ_0 such that the relative population maximum has changed from the excited state to the second one in spite of the localization (Fig. 2a). These dynamic changes in the relative eigenstate population and the fact that the eigenstate with the longest lifetime can be found anywhere in the lattice form the basis for the dynamical delocalization we discuss here. In an infinitely expanded setting, the localized eigenstates with the highest population can statistically be found at distances from the initial position that can far exceed the localization length of the eigenstates and therefore the second moment of the position operator can become unbounded, which is in stark contrast to the Hermitian case.

For strong disorder, our model allows us to analytically quantify the disorder-induced spreading of the average wavefunction.

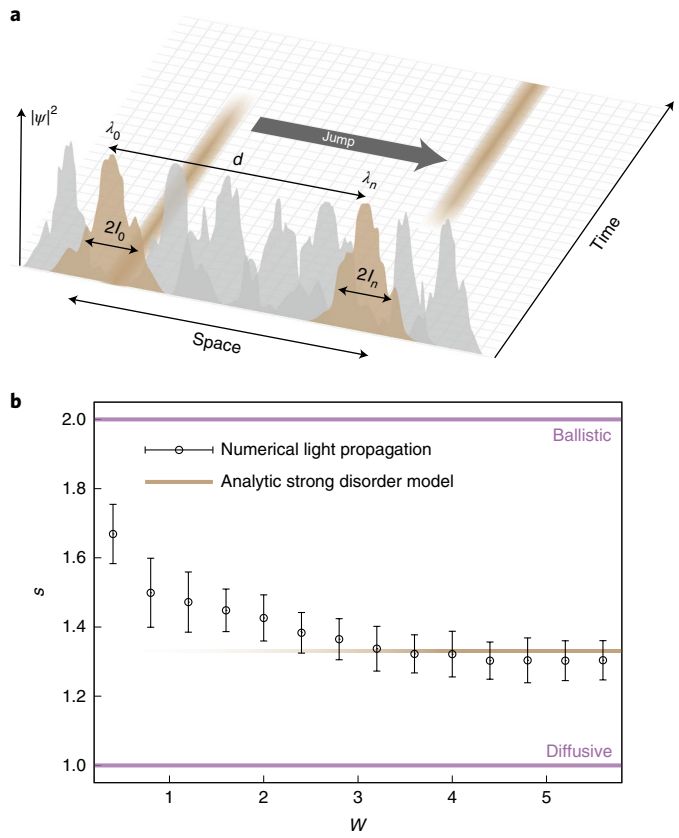

Fig. 2 | Theory of lattices with stochastic dissipation. a, Eigenstate population scheme of the analytic model. The exponentially localized eigenstates of a lattice with dissipative disorder exhibit eigenvalues λ_n with different imaginary parts. Initially, the left state is dominant. If $\mathrm{Im}(\lambda_n) > \mathrm{Im}(\lambda_0)$, the state at site n will become dominant at some time t_{change}, which depends on the localization lengths l_0, l_n and the distance d of the two states. Around t_{change}, there is a rapid spatial transition of the most dominantly populated eigenstate from the left to the right. **b**, Analytically (equation (2)) and numerically (equations (3) and (4)) extracted spreading coefficient $s(W)$ as a function of the non-Hermitian disorder strength W. Our analytical predictions agree very well with the numerical data for strong disorder, where the model assumptions hold. The error bars (see Supplementary Section 4) capture ±1 s.d. of $s(W)$. For weaker disorder, our numerical data suggest that the spreading coefficient increases as the eigenstates become less localized. Ballistic and diffusive spreading are shown for comparison.

To this end, we compute the probability $P_n(t)$ that the population maximum has changed from an initial lattice site $n=0$ to a site n at time t. Due to the stochastic dissipation, the imaginary parts of the eigenvalues are randomly distributed and follow a distribution function $f(\rho)$. The probability of a transition of the population maximum to position n, where the state has an imaginary part of the eigenvalue in the range $(\rho,\rho+\mathrm{d}\rho)$, is then determined by the joint probabilities that all other states $j\neq n$ are not dominant yet, hence $\mathrm{Im}(\lambda_j)t - |j|/l_c < \rho t - |n|/l_c$. Here, we assume that the imaginary parts of the eigenvalues of different states are independent stochastic variables with the same distribution $f(\rho)$. This assumption is particularly valid as long as the eigenstates extent only over a few sites, which is the case for strong and uncorrelated disorder. The transition probability can then be calculated via

$$P_n(t) = \int_{\frac{|n|}{tl_c}}^{\infty} \mathrm{d}\rho f(\rho) \prod_{j=0,\pm1,\pm2,\pm3\ldots\neq n} \int_{-\infty}^{\rho+\frac{|j|-|n|}{tl_c}} \mathrm{d}\rho f(\rho)\,. \qquad (2)$$

The product of the inner integrals represents the probability that all other states $j\neq n$ have a decay rate smaller than ρ. The outer integral takes into account the probability that the considered state at distance n and time t has an eigenvalue ρ that is large enough to observe the transition of the population maximum within the observation time. Note that $P_n(t)$, and hence the spatial wave spreading, is determined by $f(\rho)$. Importantly, we did not use a specific lattice structure for the derivation of equation (2) and therefore this expression should hold true for a variety of different settings. The presence of stochastic dissipation can provide the exponential localization of states and also determines a non-trivial distribution function $f(\rho)$.

As a common quantity with which to characterize the wave spreading, we consider the time evolution of the second moment $M_2(t) = \sum_n n^2 |\psi_n(t)|^2$ for a wave packet that is initially localized at $n=0$. Here $|\psi_n(t)|^2$ is the normalized population at site n (not to be confused with the nth eigenstate). Since disorder is by its nature stochastic, we employ statistical tools to capture underlying physics. We therefore consider the average second moment, which can be calculated via $\langle M_2(t)\rangle = \sum_n n^2 P_n$, with $\langle\cdot\rangle$ denoting an averaging over a set of random disorder realizations. Its slope, the spreading coefficient $s = \frac{\mathrm{d}\log M_2(t)}{\mathrm{d}\log t}$, is a general measure of wave delocalization. For comparison, ballistic spreading is characterized by a coefficient of $s=2$, whereas for diffusive spreading one finds $s=1$. For sufficiently strong disorder, such that our assumptions hold, our analytical model yields a slope of $s\to4/3$, which is dubbed super-diffusive (Fig. 2b). The exact value of s is determined by $f(\rho)$, which, in turn, depends on the disorder implementation (Supplementary Fig. 5) such that one can obtain a triangular distribution with $s_\triangle\to4/3$ but also a rectangular distribution for which we find $s_\square\to1$. The analytical results are in excellent agreement with the numerical evaluation of equation (3), which describes our experimental platform and will be introduced below. This agreement is remarkable, especially because the analytic model and the numerical propagation are two completely independent methods for estimating s. For weak disorder, our numerical data suggest that s increases and reaches the ballistic regime when the disorder ceases (Fig. 2b). Note that while the predicted unbounded second moment of the position operator is a hallmark of diffusive behaviour, it is open to discussion whether to consider the observed (non-Hermitian) dynamical delocalization as diffusion or not. This question is rooted in the general problem of distinguishing particle motion from particle exchange in open systems and it may be solved in a generalized concept of non-Hermitian diffusion.

Now we turn to the experimental demonstration of our theoretical findings. For our studies, we employ classical light propagation in coupled optical fibre loops[43,44]. They form a 1D photonic lattice with precisely tuneable parameters as a model for the evolution of single quantum particles and wave dynamics in a variety of lattice systems[45–48]. The ability to adjust the strength of dissipation at will enables the implementation of nearly arbitrary complex potentials, especially the discussed case of stochastic dissipation. To study the interplay of eigenstate localization and wave spreading, we evaluate the light propagation that arises from single-site excitations of the lattice, which corresponds to the evolution of a single-electron wavefunction that is initially localized at a specific atom.

The working principle of our experimental platform is to let optical pulses propagate in a pair of unequally long fibre loops, which are connected by a beam splitter (Fig. 3a). A detailed discussion of the full set-up is presented in the Methods. The pulse dynamics in the loops can be mapped onto the light evolution in a 1+1D double-discrete lattice, as shown in Fig. 3b and discussed in Supplementary Section 1. The light evolution is governed by a set of coupled equations[44]

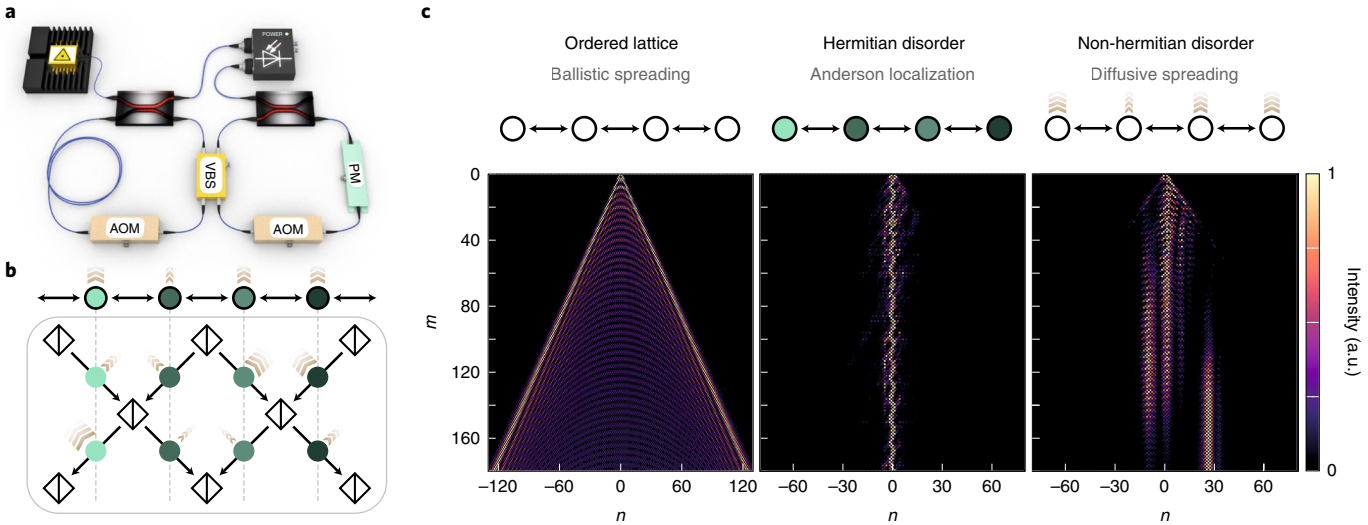

Fig. 3 | Experimental implementation of disordered lattices. a, Simplified experimental arrangement for temporally encoded lattices. Two unequally long optical fibre loops are connected by a variable beam splitter (VBS), which is set to 50:50 splitting. Acousto-optical modulators (AOMs) control the dissipation. A phase modulator (PM) controls the on-site energies. A photodetector measures the temporal light evolution. **b**, A linear chain of coupled sites (top) is realized as a 1D quantum walk (bottom). Different arrow widths correspond to different dissipation strengths. Different shades of green correspond to different on-site energies. **c**, The experimental propagation shows ballistic spreading for homogeneous lattices (left) compared to Anderson localization in Hermitian disordered lattices (centre, $W_\varphi = 0.7\pi$) at time step m and lattice position n. In the non-Hermitian case of dissipative disorder, stochastic transverse shifts of the most dominantly occupied localized state occur (right, $W_\gamma = 0.19$). a.u., arbitrary units.

$$u_n^{m+1} = \frac{G_u}{\sqrt{2}}\left(u_{n+1}^m + iv_{n+1}^m\right)\mathrm{e}^{i\varphi_u}$$
$$v_n^{m+1} = \frac{G_v}{\sqrt{2}}\left(iu_{n-1}^m + v_{n-1}^m\right) \quad (3)$$

where u_n^m denotes the amplitude at lattice position n and time step m on left-moving paths and v_n^m is the corresponding amplitude on right-moving paths. The quantities φ_u and $G_{u,v} = G_{u,v}(n, m)$ are degrees of freedom to control the imaginary and the real parts of the lattice potential, respectively. As such, our platform can model Hermitian and non-Hermitian disorder by choosing either φ_u or $G_{u,v}$ as a random variable.

Single-site excitations can be either $v_n^0 = \delta_{0n}$ or $u_n^0 = \delta_{0n}$. The squared modulus of the wavefunction $|\psi_n(t)|^2$ is represented by the normalized light intensity distribution $|u_n(t)|^2 + |v_n(t)|^2$ within the lattice. The time t corresponds to the time step m, that is $u_n(t) = u_n^m$. For the characterization of the investigated features, it is sufficient to use the light intensity distribution of one fibre loop, since the differences between the loops are only on a local scale and these vanish upon averaging, which we numerically confirmed. For this reason, all experimental data and the corresponding numerical data are based on the intensity distribution $|u_n(t)|^2$ in the u loop.

In the homogeneous, disorder-free lattice $G_u = G_v = 1$, $\varphi_u = 0$, a single-site excitation yields the well-known ballistic spreading of the wavefunction[24] (left panel of Fig. 3c). As a result, the initially localized wave packet quickly becomes delocalized and acquires a high probability to be found far away from its initial position. Now we consider the two cases with disorder. In the conventional Hermitian case, disorder is commonly realized by a time-independent but spatially random real part of the potential[49]. We realize the random changes in the real part of the potential by drawing $\varphi_u \in [-W, W]$ for each lattice site n from a uniform probability distribution with disorder strength W. In accordance to previous studies[50,51], a single-site excitation in such disordered lattice (here with $W_\varphi = 0.7\pi$) undergoes repeated scattering at the potential fluctuations, leading to a superposition of destructively interfering waves in such a way that previously extended states localize at the initial position (middle panel of Fig. 3c). This process is the Anderson localization.

Within the non-Hermitian model, disorder is represented by a stochastic energy or particle exchange with the environment; that is, random changes in the imaginary part of the potential. The imaginary potential fluctuations are given by

$$G_{u,v} = \mathrm{e}^{i\gamma},\ \gamma \in [-iW, iW] \quad (4)$$

and are also drawn from a uniform probability distribution for each lattice site. While mathematically this distribution also includes gain, the results do not depend on whether a purely passive system or a system with gain and loss is chosen, which also has been confirmed in earlier theoretical works[14]. We find, numerically, with equation (3) and in the experiments, that a single-site excitation localizes due to the non-Hermitian disorder $W_\gamma = 0.19$ (right panel of Fig. 3c), which is in agreement with the predicted localization of eigenstates. Yet, we observe a spatial change of the eigenstate population in agreement with the prediction of our theoretical model, yielding on average the dynamical delocalization. Remarkably, the distances between the dominant eigenstates can substantially exceed the localization length of the individual eigenstates. This demonstrates that in non-Hermitian systems even extremely small overlaps between the localized eigenstates can suffice to substantially influence the temporal evolution of the wavefunction. Moreover, not only the average, but also the individual experimental light evolutions, agree very well with the numerical propagation of equation (3) (Supplementary Fig. 2).

To validate the key aspects of our theoretical considerations, we study the localization properties of the populated states. To obtain the profile of the eigenstates, we measure the intensity distribution of an initially localized excitation at a large observation time. This is repeated for different disorder realizations. The acquired intensity distributions are then averaged after they are spatially shifted to share the same centre of mass to avoid the ambiguity of the positions of the populated eigenstate. The result (Fig. 4a)

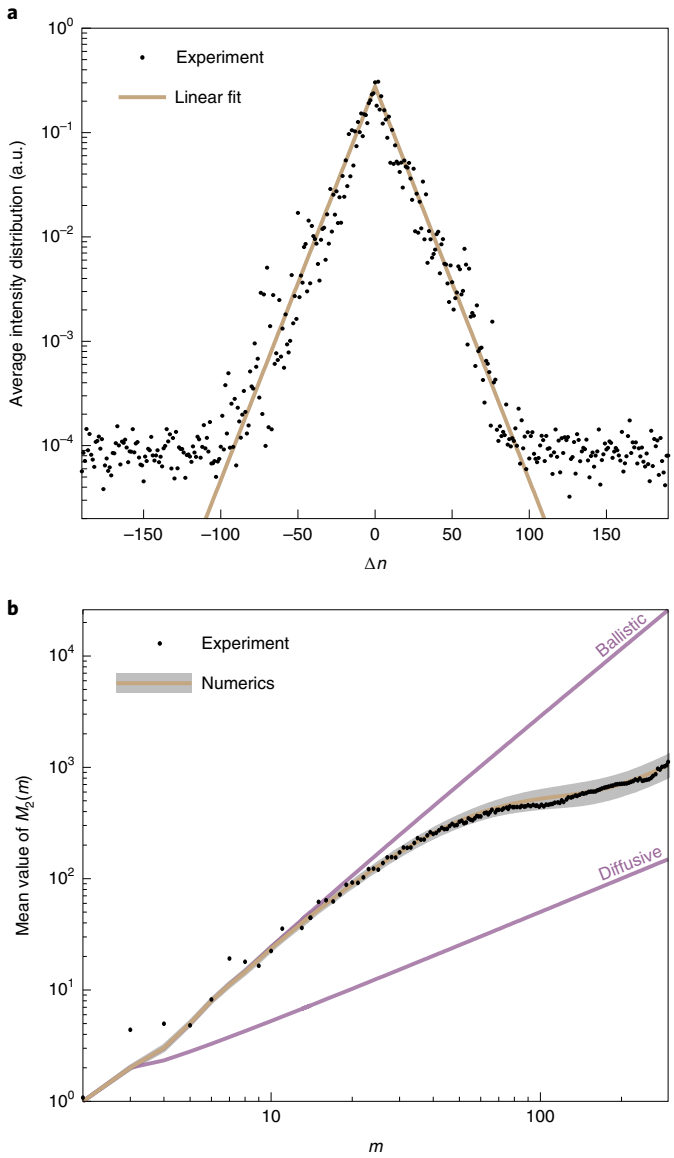

Fig. 4 | Coexistence of spectral localization and dynamical delocalization in lattices with dissipative disorder. a, Average centred intensity distribution at time step $m = 110$ and lattice position n. The experimental data clearly demonstrate the exponential localization induced by stochastic dissipation. The experimental data are based on 40 different lattices with dissipative disorder. **b**, Time evolution of the mean value of the second moment $M_2(m)$. For a large number of disorder realizations, the numerical data converge to the shown line for stochastic dissipation. The grey area shows ±1 s.d. of expected statistical fluctuations, which arise from using only 40 disorder realizations instead of a much larger set. Ballistic and diffusive spreading are shown for comparison. The experimental and numerical data are obtained for the case of a fixed disorder strength $W_y = 0.19$; the dependency of s on W can be found in Fig. 2b.

clearly shows the exponential localization by a linear decay in the logarithmic scale.

In the next step, we quantify the properties of the average wave spreading that occurs due to the population changes of the exponentially localized states. Therefore, we evaluate the time evolution of the second moment $M_2(t)$ for an excitation initially localized at $n = 0$. Here, $M_2(t)$ is a random variable that changes with every disorder realization. Consequently, the data that are extracted from the experiments contain the second moments of different disorder realizations, from which we then derive the mean $\langle M_2(t)\rangle$ and the standard deviation $\sigma(M_2(t))$. These quantities allow us to draw statistically meaningful conclusions for the spatial spreading of the wavefunction. In Supplementary Section 3, we also evaluate the statistical movement of the wavefunction's centre of mass to further characterize the change in the eigenstate population.

The experimental results (Fig. 4b) clearly demonstrate that the average wave spreading in the presence of non-Hermitian disorder can fundamentally differ from the Hermitian case, even though in both cases all eigenstates are exponentially localized. Furthermore, the experimental data successfully match the numerical results obtained from equation (3) within the range of 1 s.d. of the expected statistical fluctuations. From the monotonic increase of $M_2(t)$, one can conclude that the dissipative disorder facilitates a spreading coefficient of the average wavefunction comparable to a super-diffusive system, which is in strong contrast to the Hermitian case, where the mean of the second moment quickly saturates and the average wavefunction is predetermined to remain localized forever at its initial position.

These results pose the question of what happens when both the real and the imaginary parts of the potential are subject to random changes. Uncorrelated disorder in the real part of the potential leads to Anderson localization and completely suppresses transport, whereas uncorrelated disorder in the imaginary part of the potential can induce spreading through dynamical delocalization. Our experimental data show that the spectral localization, initially induced by Anderson localization, does not necessarily lead to a suppression of non-Hermitian wave spreading as the stochastic dissipation still facilitates a change in the eigenstate population (Supplementary Fig. 7). Furthermore, while our results lay the foundation for 1D systems with non-Hermitian disorder, recent theoretical studies investigate a possible Anderson localization transition in 3D systems with non-Hermitian disorder[22,52].

A hallmark of the Hermitian Anderson model with uncorrelated disorder is the equivalence between spectral localization and dynamical localization[37,38], that is, exponential localization of all eigenstates by uncorrelated on-site potential disorder implies the absence of wave spreading in the lattice and vice versa. Here we predicted and observed, using a photonic lattice platform, the breakdown of this equivalence caused by uncorrelated stochastic dissipation. We further experimentally demonstrated that stochastic dissipation not only facilitates wave spreading but can also simultaneously be the origin of spectral localization. Our results can be applied in principle to numerous platforms beyond photonics, such as matter waves, acoustic waves and electrons. As every real-world system is subject to dissipation and disorder, we anticipate that our findings will inspire an extended understanding and control of localization and wave spreading in a variety of classical and quantum physical settings. Furthermore, we anticipate that the illuminated links between the observed spatial spreading and conventional (Hermitian) diffusion could contribute to the development of a new and generalized non-Hermitian concept of diffusion.

Online content

Any methods, additional references, Nature Research reporting summaries, source data, extended data, supplementary information, acknowledgements, peer review information; details of author contributions and competing interests; and statements of data and code availability are available at https://doi.org/10.1038/s41566-021-00823-w.

Received: 16 September 2020; Accepted: 30 April 2021;
Published online: 17 June 2021

References

1. Anderson, P. W. Absence of diffusion in certain random lattices. *Phys. Rev.* **109**, 1492–1505 (1958).
2. Lagendijk, A., van Tiggelen, B. & Wiersma, D. S. Fifty years of Anderson localization. *Phys. Today* **62**, 24–29 (2009).
3. Datta, S. *Electronic Transport in Mesoscopic Systems* (Cambridge Univ. Press, 1995).
4. Abrahams, E. *50 Years of Anderson Localization* (World Scientific Publishing Co., 2010).
5. Segev, M., Silberberg, Y. & Christodoulides, D. N. Anderson localization of light. *Nat. Photon.* **7**, 197–204 (2013).
6. Schwartz, T., Bartal, G., Fishman, S. & Segev, M. Transport and Anderson localization in disordered two-dimensional photonic lattices. *Nature* **446**, 52–55 (2007).
7. Sapienza, L. et al. Cavity quantum electrodynamics with Anderson-localized modes. *Science* **327**, 1352–1355 (2010).
8. Wiersma, D. S. The physics and applications of random lasers. *Nat. Phys.* **4**, 359–367 (2008).
9. Stano, P. & Jacquod, P. Suppression of interactions in multimode random lasers in the Anderson localized regime. *Nat. Photon.* **7**, 66–71 (2013).
10. Li, J., Chu, R. L., Jain, J. K. & Shen, S. Q. Topological Anderson insulator. *Phys. Rev. Lett.* **102**, 136806 (2009).
11. Meier, E. J. et al. Observation of the topological Anderson insulator in disordered atomic wires. *Science* **362**, 929–933 (2018).
12. Stützer, S. et al. Photonic topological Anderson insulators. *Nature* **560**, 461–465 (2018).
13. Mott, N. F. & Davis, E. A. *Electronic Processes in Non-Crystalline Materials* (Clarendon Press, 1979).
14. Basiri, A., Bromberg, Y., Yamilov, A., Cao, H. & Kottos, T. Light localization induced by a random imaginary refractive index. *Phys. Rev. A* **90**, 043815 (2014).
15. Hatano, N. & Nelson, D. R. Localization transitions in non-Hermitian quantum mechanics. *Phys. Rev. Lett.* **77**, 570–573 (1996).
16. Hamazaki, R., Kawabata, K. & Ueda, M. Non-Hermitian many-body localization. *Phys. Rev. Lett.* **123**, 090603 (2019).
17. Yusipov, I., Laptyeva, T., Denisov, S. & Ivanchenko, M. Localization in open quantum systems. *Phys. Rev. Lett.* **118**, 070402 (2017).
18. Yusipov, I. I., Laptyeva, T. V. & Ivanchenko, M. V. Quantum jumps on Anderson attractors. *Phys. Rev. B* **97**, 020301 (2018).
19. Balasubrahmaniyam, M., Mondal, S. & Mujumdar, S. Necklace-state-mediated anomalous enhancement of transport in Anderson-localized non-Hermitian hybrid systems. *Phys. Rev. Lett.* **124**, 123901 (2020).
20. Tzortzakakis, A. F., Makris, K. G. & Economou, E. N. Non-Hermitian disorder in two-dimensional optical lattices. *Phys. Rev. B* **101**, 014202 (2020).
21. Yamilov, A. G. et al. Position-dependent diffusion of light in disordered waveguides. *Phys. Rev. Lett.* **112**, 023904 (2014).
22. Huang, Y. & Shklovskii, B. I. Anderson transition in three-dimensional systems with non-Hermitian disorder. *Phys. Rev. B* **101**, 014204 (2020).
23. Drude, P. *Zur Elektronentheorie der Metalle. Ann. Phys.* **306**, 566–613 (1900).
24. Bloch, F. *Über die Quantenmechanik der Elektronen in Kristallgittern. Z. Phys.* **52**, 555–600 (1929).
25. Pascual, J. I. et al. Properties of metallic nanowires: from conductance quantization to localization. *Science* **267**, 1793–1795 (1995).
26. Ying, T. et al. Anderson localization of electrons in single crystals: $Li_xFe_7Se_8$. *Sci. Adv.* **2**, e1501283 (2016).
27. Billy, J. et al. Direct observation of Anderson localization of matter waves in a controlled disorder. *Nature* **453**, 891–894 (2008).
28. Roati, G. et al. Anderson localization of a non-interacting Bose–Einstein condensate. *Nature* **453**, 895–898 (2008).
29. Hu, H., Strybulevych, A., Page, J. H., Skipetrov, S. E. & van Tiggelen, B. A. Localization of ultrasound in a three-dimensional elastic network. *Nat. Phys.* **4**, 945–948 (2008).
30. Hatano, N. & Nelson, D. R. Non-Hermitian delocalization and eigenfunctions. *Phys. Rev. B* **58**, 8384–8390 (1998).
31. Laptyeva, T. V., Tikhomirov, A. A., Kanakov, O. I. & Ivanchenko, M. V. Anderson attractors in active arrays. *Sci. Rep.* **5**, 13263 (2015).
32. van Tiggelen, B. A., Lagendijk, A. & Wiersma, D. S. Reflection and transmission of waves near the localization threshold. *Phys. Rev. Lett.* **84**, 4333–4336 (2000).
33. Wang, J. & Genack, A. Z. Transport through modes in random media. *Nature* **471**, 345–349 (2011).
34. Tian, C. S., Cheung, S. K. & Zhang, Z. Q. Local diffusion theory for localized waves in open media. *Phys. Rev. Lett.* **105**, 263905 (2010).
35. Pendry, J. B. Quasi-extended electron states in strongly disordered systems. *J. Phys. C* **20**, 733 (1987).
36. Bertolotti, J., Gottardo, S., Wiersma, D. S., Ghulinyan, M. & Pavesi, L. Optical necklace states in Anderson localized 1D systems. *Phys. Rev. Lett.* **94**, 113903 (2005).
37. Del Rio, R., Jitomirskaya, S., Last, Y. & Simon, B. What is localization? *Phys. Rev. Lett.* **75**, 117–119 (1995).
38. Bucaj, V. et al. Localization for the one-dimensional Anderson model via positivity and large deviations for the Lyapunov exponent. *Trans. Am. Math. Soc.* **372**, 3619–3667 (2019).
39. Phillips, P. & Wu, H. L. Localization and its absence: a new metallic state for conducting polymers. *Science* **252**, 1805–1812 (1991).
40. Xiao, L. et al. Observation of topological edge states in parity–time-symmetric quantum walks. *Nat. Phys.* **13**, 1117–1123 (2017).
41. Eichelkraut, T. et al. Mobility transition from ballistic to diffusive transport in non-Hermitian lattices. *Nat. Commun.* **4**, 2533 (2013).
42. Klauck, F. et al. Observation of PT-symmetric quantum interference. *Nat. Photon.* **13**, 883–887 (2019).
43. Schreiber, A. et al. Photons walking the line: a quantum walk with adjustable coin operations. *Phys. Rev. Lett.* **104**, 050502 (2010).
44. Regensburger, A. et al. Parity–time synthetic photonic lattices. *Nature* **488**, 167–171 (2012).
45. Wimmer, M., Price, H. M., Carusotto, I. & Peschel, U. Experimental measurement of the Berry curvature from anomalous transport. *Nat. Phys.* **13**, 545–550 (2017).
46. Muniz, A. L. M. et al. 2D solitons in *PT*-symmetric photonic lattices. *Phys. Rev. Lett.* **123**, 253903 (2019).
47. Bisianov, A., Wimmer, M., Peschel, U. & Egorov, O. A. Stability of topologically protected edge states in nonlinear fiber loops. *Phys. Rev. A* **100**, 063830 (2019).
48. Weidemann, S. et al. Topological funneling of light. *Science* **368**, 311–314 (2020).
49. Kramer, B. & MacKinnon, A. Localization: theory and experiment. *Rep. Prog. Phys.* **56**, 1469–1564 (1993).
50. Regensburger, A. et al. Photon propagation in a discrete fiber network: an interplay of coherence and losses. *Phys. Rev. Lett.* **107**, 233902 (2011).
51. Derevyanko, S. Anderson localization of a one-dimensional quantum walker. *Sci. Rep.* **8**, 1795 (2018).
52. Luo, X., Ohtsuki, T. & Shindou, R. Universality classes of the Anderson transitions driven by non-Hermitian disorder. *Phys. Rev. Lett.* **126**, 090402 (2021).

Methods

Experimental set-up. Each experimental run starts by injecting a single 50 ns pulse into the longer fibre loop, which is coupled to a shorter fibre loop by a 50:50 beam splitter (Fig. 3a). The input pulse is cut out of a continuous wave signal from a distributed feedback laser (JDS Uniphase, 1,550 nm) with a Mach–Zehnder intensity modulator (SDL Integrated Optics Limited). An acousto-optical modulator is then used as a pulse picker. In the coupled fibre loops, the initial pulse repeatedly splits at the central beam splitter and, after several round trips, multipath interference between the emerging sub-pulses takes place. In each fibre loop an acousto-optical modulator (Brimrose) is placed to manipulate the pulse amplitudes, which allows us to emulate the disordered dissipation. The outputs of the acousto-optical modulators are aligned to the 0th diffraction order to avoid frequency shifts of the propagating light. Light is injected into the loops or coupled out by fused fibre couplers (AC Photonics). The light intensity is measured using photodetectors (Thorlabs). Single mode fibres (Corning Vascade LEAF EP) were used to extend the propagation time for each loop to approximately 27 µs. By adding a fibre optic patch cable in one of the loops, a 70–120 ns difference in propagation time is induced, such that one has a long and a short loop. A phase modulator (iXblue Photonics) in the shorter loop manipulates the phase of propagating pulses and thereby controls the real part of the lattice potential. An erbium-doped fibre amplifier (Thorlabs) in each loop compensates for propagation losses (for example, insertion losses and detection losses) and allows us to maintain a high optical signal-to-noise ratio. The amplification scheme is balanced between both loops such that the multipath interference is not altered. The fibre amplifiers are optically gain clamped by injecting a high-power continuous wave laser signal (JDS Uniphase, 1,538 nm) into the amplifier via a wavelength division multiplexing coupler (AC Photonics). Bandpass filters (WL Photonics) suppress optical noise from the amplified spontaneous emission and remove the laser signal that was injected for the optical gain clamping. All fibre components are designed for operation at 1,550 nm wavelength and employ standard single mode fibres, for example SMF28 or comparable. The polarization state of the propagating light is controlled via mechanical polarization controllers. The polarization needs to be aligned in front of polarization-sensitive components to obtain a high interference contrast. Arbitrary waveform generators (Keysight Technologies, 33,622 A) generate all electrical signals that drive the modulators.

Data acquisition. To measure the statistical behaviour of the wave dynamics in the presence of dissipative disorder, 40 random realizations of dissipative disorder were generated in MATLAB and then converted into a waveform signal, which is applied to the amplitude modulators by the arbitrary waveform generators. To obtain the squared modulus of the lattice site amplitudes in the presented datasets, we performed a time-resolved measurement of pulse intensities with a photodiode (Thorlabs) in the shorter fibre loop. The output voltages of the photodiode are amplified with a logarithmic amplifier (FEMTO HLVA-100) and afterwards sampled with an oscilloscope (R&S RTO1104). With the time scales Δt and T of the fibre loop arrangement, one can map the acquired voltage signal onto the discrete 1 + 1D grid (m,n) in which the measured pulse intensities represent the squared modulus of the lattice site amplitude for the respective propagation step m and lattice position n. Each measurement features an additional noise measurement in which the lattice excitation is turned off. In the post-processing, these noise data are subtracted from the data in which the lattice was excited.

Data availability

All experimental data that have been used to produce the results reported in this manuscript are available in an open-access data repository[53].

References

53. Weidemann, S., Kremer, M., Longhi, S. & Szameit, A. Dataset for 'Coexistence of dynamical delocalization and spectral localization through stochastic dissipation'. Rostock University Publication Server https://doi.org/10.18453/rosdok_id00002990 (2021).

Acknowledgements

S.W., M.K. and A.S. thank the Deutsche Forschungsgemeinschaft (grant SZ 276/20-1) and the Krupp von-Bohlen-and-Halbach foundation for funding their research. S.L. acknowledges the Spanish State Research Agency through the Severo Ochoa and Maria de Maeztu Program for Centers and Units of Excellence in R&D (MDM-2017-0711).

Author contributions

S.W. and M.K. designed the experimental implementation. S.W. performed the experiments. S.L. developed the analytical model. A.S. supervised the project. All authors discussed the results and co-wrote the manuscript.

Competing interests

The authors declare no competing interests.

Additional information

Supplementary information The online version contains supplementary material available at https://doi.org/10.1038/s41566-021-00823-w.

Correspondence and requests for materials should be addressed to A.S.

Peer review information *Nature Photonics* thanks Diederik Wiersma and the other, anonymous, reviewer(s) for their contribution to the peer review of this work.

Reprints and permissions information is available at www.nature.com/reprints.